Optica Applicata, Vol. LII, No. 4, 2022
DOI: 10.37190/oa220405

Modeling and evaluation of performance of dual field-of-view common-aperture dual-band imaging system

QINGSONG WANG, MING GAO

College of Optoelectronic Engineering, Xi'an Technological University,
Xi'an, Shaanxi 710021, China

For the modeling and evaluation of dual field-of-view (FOV) common-aperture dual-band imaging system performance, two factors must be considered at the same time. One is that the system must have a larger target acquisition range, and the other is that the detection range and recognition range of the system must be the same. In this paper, taking the dual FOV common-aperture visible/long-wave infrared (LWIR) imaging system as an example, the performance of the dual FOV common-aperture dual-band imaging system is modeled and evaluated using an imaging system performance model based on comprehensive resolution. Firstly, the target acquisition range of the dual FOV visible imaging system is analyzed, and the condition that the detection range is equal to the recognition range is obtained. Then, under the condition of common aperture, the target acquisition range and the relationship between detection range and recognition range of dual FOV LWIR imaging system are analyzed. The analysis results show that, under the condition of dual FOV and common aperture, when the detection and recognition ranges of the visible imaging system are equal, the detection and recognition ranges of the LWIR imaging system are not equal. When the detection and recognition ranges are close by reducing the comprehensive resolution, the target acquisition range of the dual FOV common-aperture dual-band imaging system will decrease.

Keywords: common-aperture, dual-band, dual FOV, performance modeling.

1. Introduction

Dual-band imaging has the advantage of complementary scene information. In addition, it has been highly valued in the military, security, agriculture and other fields [1,2]. The combination of visible imaging and LWIR imaging is a typical dual-band imaging form. The reason is that visible imaging has the advantage of high resolution compared with LWIR imaging. However, LWIR imaging has the advantage of strong penetration and is not affected by ambient light. Usually two independent single-band imaging systems are integrated to achieve dual-band imaging. The dual-band imaging system has the characteristics of light weight, small volume and simple image fusion algorithm

after adopting the common-aperture structure [3–6]. The dual FOV is usually used to realize the detection task and the recognition task in the target acquisition task, which is to identify the target by adjusting the wide field-of-view (WFOV) to a narrow field-of-view (NFOV) without changing the position of the observer [7]. As a consequence, two factors should be considered at the same time when modeling and evaluating the performance of the dual FOV common-aperture dual-band imaging system. One is that the system should have a large target acquisition range (collectively referred to as the detection range and the recognition range). Second, the detection range of the system should be the same as the recognition range.

The United States Army uses the night vision integrated performance model (NVIPM) based on targeting task performance (TTP) metric to model and evaluate the performance of the imaging system [8,9]. NVIPM is a very complex physical model related to many factors. By using the approximation of NVIPM based on the comprehensive resolution, and combined with the characteristics of common aperture and dual FOV, the relationship between target acquisition range, detection range and recognition range of visible/LWIR imaging system is modeled and evaluated.

2. Performance evaluation model

The TTP metric in NVIPM is related to the parameters describing imaging system, target characteristics, atmospheric conditions, display and eyes, *etc*. The TTP metric defined as [10,11]

$$M_{\mathrm{TTP}} = \int_{u_{\mathrm{L}}}^{u_{\mathrm{H}}} \sqrt{\frac{C_{\mathrm{T}}}{C_{\mathrm{S}}(u)}}\,\mathrm{d}u = \int_{u_{\mathrm{L}}}^{u_{\mathrm{H}}} \sqrt{\frac{C_{\mathrm{T}}}{\dfrac{C_{\mathrm{E}}(u)}{M_{\mathrm{S}}(u)}\left(1+\dfrac{\alpha^2 N^2(u)}{L^2}\right)^{1/2}}}\,\mathrm{d}u \tag{1}$$

where M_{TTP} is the TTP metric in cycles/mrad, u is the spatial frequency in cycles/mrad, $C_{\mathrm{S}}(u)$ is the contrast threshold function of the imaging system, $C_{\mathrm{E}}(u)$ is the contrast threshold function of the eye, $M_{\mathrm{S}}(u)$ is the modulation transfer function of the imaging system, $N(u)$ is the display rms noise, α is the empirical constant, L is the brightness of the display in foot Lambert (fL), C_{T} is the contrast of the target on the display, u_{H} and u_{L} are the spatial frequencies corresponding to the intersection of C_{T} and $C_{\mathrm{S}}(u)$ in cycles/mrad.

In NVIPM, if the target contrast, the characteristic dimension of the target, the target acquisition task and the number of cycles on the target are given, the target acquisition range is

$$R = \frac{W_{\mathrm{T}}}{N} M_{\mathrm{TTP}} \tag{2}$$

where, R is the target acquisition range (km); W_T is the characteristic dimension of the target (m); N is the number of cycles on the target, which is related to the probability of completing the target acquisition task.

It can be concluded from Eq. (1), that Eq. (2) is a very complex performance model. When neglecting atmospheric transmittance and imaging system signal-to-noise ratio (SNR), it can be approximated by [12, 13]

$$R \approx \frac{W_T}{N} K V_{FOM} \frac{D}{\lambda} \tag{3}$$

where D is the diameter of the clear aperture of the optical system in mm, λ is the wavelength in μm, K is the calibration coefficient, which is related to the brightness of the display and the target contrast on the display, and V_{FOM} is the figure of merit (FOM), which is expressed as

$$V_{FOM} \approx \int_0^{u_n} \sqrt{\frac{M_O(u) M_D(u) M_{FP}(u)}{C_E(u)}}\, du \tag{4}$$

where u_n is the Nyquist frequency in cycles/mrad, $M_O(u)$, $M_D(u)$ and $M_{FP}(u)$ are the modulation transfer functions of optical systems, detectors and flat panel displays, respectively.

The comprehensive resolution Q [12, 13] is defined as the ratio of the detector cutoff frequency to the optical cutoff frequency,

$$Q = \frac{u_D}{u_O} = \frac{f'\lambda}{Dd} = \frac{F\lambda}{d} \tag{5}$$

where u_O and u_D are the cutoff frequencies of the optical system and the detector in cycles/mrad, respectively, f' is the focal length of the optical system in mm, d is the detector size in μm, and F is f-number.

For target detection task and recognition task, the Eq. (4) fit valid up to $Q = 4$ [14] provides:

$$V_{FOM\_D} \approx a_6 Q^6 + a_5 Q^5 + a_4 Q^4 + a_3 Q^3 + a_2 Q^2 + a_1 Q \tag{6}$$

$$V_{FOM\_R} \approx b_6 Q^6 + b_5 Q^5 + b_4 Q^4 + b_3 Q^3 + b_2 Q^2 + b_1 Q \tag{7}$$

where V_{FOM_D} and V_{FOM_R} are the FOMs of detection and identification, respectively. $a_6 = -0.00249$, $a_5 = 0.02546$, $a_4 = -0.008275$, $a_3 = 0.08981$, $a_2 = -0.16979$, $a_1 = 0.82954$, $b_6 = -0.00247$, $b_5 = 0.0261$, $b_4 = -0.0901$, $b_3 = 0.1098$, $b_2 = -0.1582$, and $b_1 = 0.7402$.

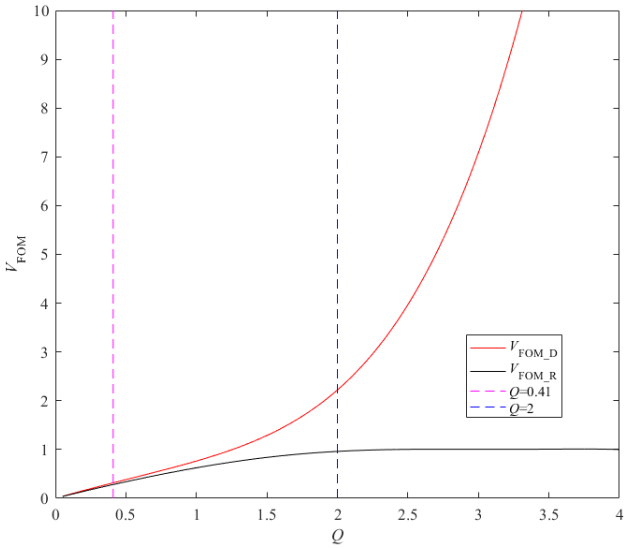

Fig. 1. Relationship between V_{FOM_D} and V_{FOM_R} and Q.

The curve of the relationship between V_{FOM_D} and V_{FOM_R} and Q is shown in Fig. 1. Based on the definition of Q, the curve can be divided into three regions: the detector -limited region for $Q \leq 0.41$, the transition region for $0.41 < Q < 2$ and the optics-limited region for $2 \leq Q \leq 4$.

3. Performance of dual FOV visible imaging system

3.1. Target acquisition range of dual FOV visible imaging system

The equations of detection range and recognition range of visible imaging system can be obtained from Eqs. (3), (6) and (7).

$$R_{D\_V} \approx \frac{W_T}{N_D} K V_{FOM\_D\_V} \frac{D_D}{\lambda_V} \tag{8}$$

$$R_{R\_V} \approx \frac{W_T}{N_R} K V_{FOM\_R\_V} \frac{D_R}{\lambda_V} \tag{9}$$

where R_{D_V} and R_{R_V} are the detection range and recognition range of the visible imaging system in km, respectively, $V_{FOM\_D\_V}$ and $V_{FOM\_R\_V}$ are the FOM of the detection and recognition of the visible imaging system, respectively; D_D and D_R are the diameters of the clear aperture for detection and recognition in mm, respectively, λ_V is the average wavelength of visible, $\lambda_V = 0.55$ μm, N_D and N_R are the number of cycles on the target when the detection and recognition probability is 50%, respectively. $N_D = 2.0$, $N_R = 7.5$, $W_T = 3.11$ m are recommended in NVIPM.

3.1.1. The relationship between target acquisition range and focal length, clear aperture and detector size

For the convenience of discussion, assume the focal length of the optical system changes between 20 and 200 mm, the diameter of the clear aperture changes between 25 and 100 mm, and the F changes between 0.5 and 8. When the size of the visible detector d_V is 3.5 and 5 μm, respectively, the relationship between the target acquisition range and the focal length, the diameter of the clear aperture and the size of the detector calculated by the Eqs. (6)–(9) is shown in Fig. 2. Figure 2 shows that the target acquisition range increases with the increase of the focal length and the decrease of the detector size. When the focal length is small, the diameter of the clear aperture has little effect on the target acquisition range, but when the focal length is large, the diameter of the clear aperture has a certain effect on the target acquisition range. There is an interval between the detection range and the recognition range (the area between the maximum recognition range and the minimum detection range in Fig. 2). In addition, the equal interval increases with the increase of the focal length range and the decrease of the detector size.

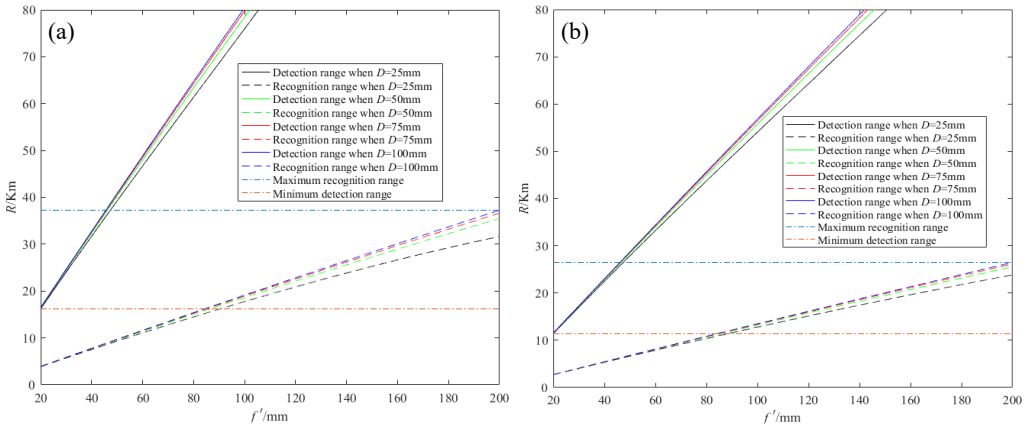

Fig. 2. Relationship between the target acquisition range of the visible imaging system and the focal length, clear aperture, and detector size. (a) d_V = 3.5 μm, and (b) d_V = 5 μm.

3.1.2. The influence of F on target acquisition range

Figure 3 shows the relationship between the F and the interval where the target acquisition range and the detection range are equal to the recognition range. As can be seen from Fig. 3, the F corresponding to the interval in which the target acquisition range and detection range are equal to the recognition range is between 0.5 and 8, which is limited by the SNR and sensitivity of the imaging system. In fact, the F cannot be taken to such a large range. Figure 3 also shows the corresponding target acquisition range and the interval where the detection range and the recognition range are equal when F = 1 and F = 4. Figure 3 shows that the F has a great influence on the target acqui-

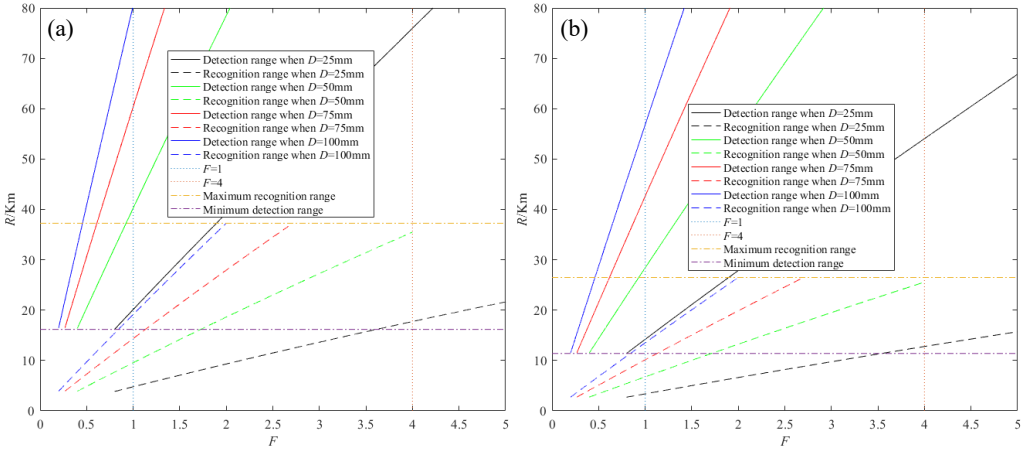

Fig. 3. Relationship between the target acquisition range of the visible imaging system and the F number. (a) $d_V = 3.5$ μm, and (b) $d_V = 5$ μm.

sition performance for the imaging system with small clear aperture, which is shown in that the F reduces the maximum value of the target acquisition range; in the case of the same F, the smaller the size of the detector, the larger the target acquisition range. When the F of detection and recognition is the same, the F has a great influence on the interval where the detection range is equal to the recognition range. As can be seen from Fig. 3, if the detection range is equal to the recognition range, the diameter of the clear aperture at the time of detection is either reduced or the diameter of the clear aperture at the time of identification is increased if the detection range is equal to the recognition range. It is almost impossible for the detection range to be equal to the recognition range when $F = 4$ is used, because the minimum detection range is much larger than the maximum recognition range.

3.1.3. The relationship between target acquisition range and comprehensive resolution

The relationship between the target acquisition range and the interval where the detection range is equal to the recognition range and the comprehensive resolution Q_V is shown in Fig. 4. Figure 4 shows that the target acquisition range increases with the increase of the comprehensive resolution; due to the influence of the F, the upper limit of the comprehensive resolution is usually limited to the value corresponding to $F = 4$, so for the smaller clear aperture, the larger target acquisition range corresponding to the larger comprehensive resolution has no practical significance. When the comprehensive resolution of detection and recognition is the same, the comprehensive resolution has a great influence on the interval where the detection range is equal to the recognition range. It can be seen from the Fig. 4 that the smaller the comprehensive resolution, the smaller the difference between the detection range and the recognition range. In

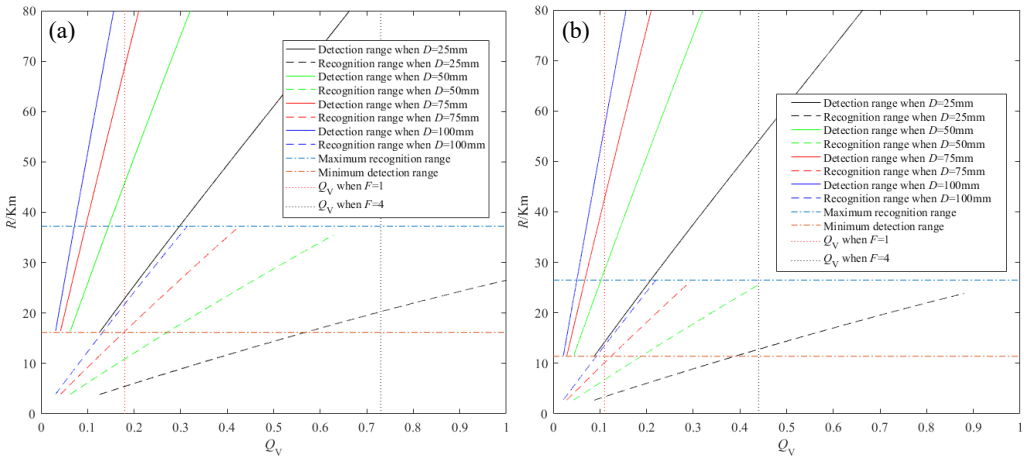

Fig. 4. Relationship between the target acquisition range of the visible imaging system and the comprehensive resolution. (a) d_V = 3.5 μm, and (b) d_V = 5 μm.

fact, it contradicts the requirement that the target acquisition range requires a larger comprehensive resolution.

3.2. The condition that the detection range is equal to the recognition range of the dual FOV visible imaging system

As can be seen from Eq. (5), the first five terms in Eqs. (6) and (7) will become very small, and Eqs. (8) and (9) can be approximated as

$$R_{D\_V} \approx a_1 \frac{W_T}{N_D} K \frac{f'_D}{d_V} \tag{10}$$

$$R_{R\_V} \approx b_1 \frac{W_T}{N_R} K \frac{f'_R}{d_V} \tag{11}$$

where f'_D and f'_R are the focal length for detection and recognition, respectively.

Equations (10) and (11) show that when the comprehensive resolution is very small, there is almost no relationship between the target acquisition range and the clear aperture, which is consistent with Fig. 2.

From Eqs. (10) and (11), the condition that the detection range is equal to the recognition range is

$$\frac{a_1 f'_D}{N_D} = \frac{b_1 f'_R}{N_R} \tag{12}$$

From Eq. (12), the relationship between the focal length when the detection range is equal to the recognition range is shown in Table 1. The subscript D and R in the table

T a b l e 1. Relationship between focal length, clear aperture, IFOV and comprehensive resolution during detection and recognition.

f' [mm]	$f'_R = 4.2\, f'_D$
D [mm]	$D_R = 4.2\, D_D$
W [mrad]	$W_R = 0.24\, W_D$
F	$F_R = F_D$
Q	$Q_R = Q_D$

represent detection and identification, respectively. Table 1 also shows the relationship between the diameter of the clear aperture, the instantaneous field-of-view (IFOV) W, and the comprehensive resolution in detection and recognition. Table 1 shows that when the focal length of the optical system, the diameter of the clear aperture, the IFOV, the F, and the comprehensive resolution during detection are respectively 4.2, 4.2, 0.24, 1 and 1, times the corresponding parameters during identification, the detection range is equal to the recognition range.

4. Performance of dual FOV LWIR imaging system

4.1. Target acquisition range of dual FOV LWIR imaging system

The relationship between the target acquisition range of the LWIR imaging system and the aperture, focal length and detector size of the LWIR imaging system can be obtained based on Eqs. (3), (6) and (7), as shown in Fig. 5. The detectors size d_{LWIR} in Fig. 5(a)–(d) and (e)–(h) are 12 and 17 μm, respectively. The average wavelength of the LWIR is 10 μm in Fig. 5. Figure 5 shows that the target acquisition range increases

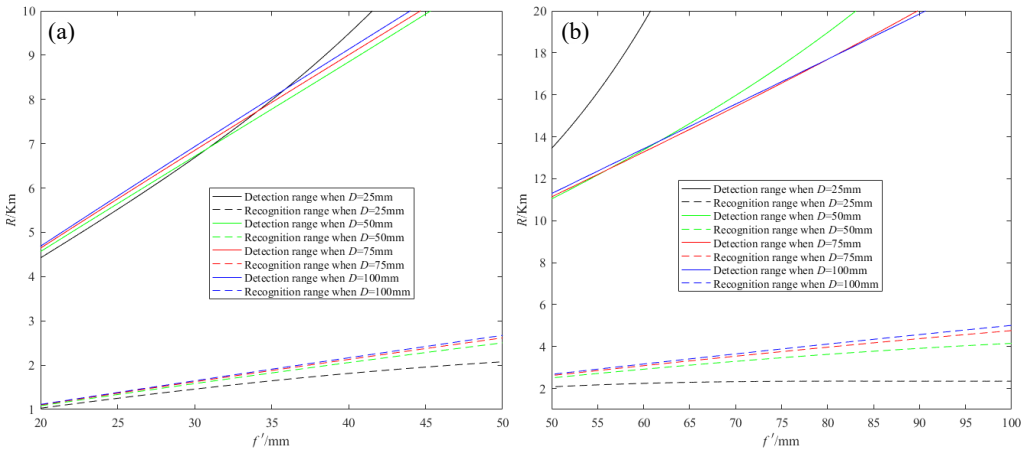

Fig. 5. Relationship between the target acquisition range of the LWIR imaging system and the clear aperture, focal length and detector size. (a, e) f' = 20...50 mm, (b, f) f' = 50...100 mm, (c, g) f' = 100...200 mm, (d, h) f' = 20...200 mm.

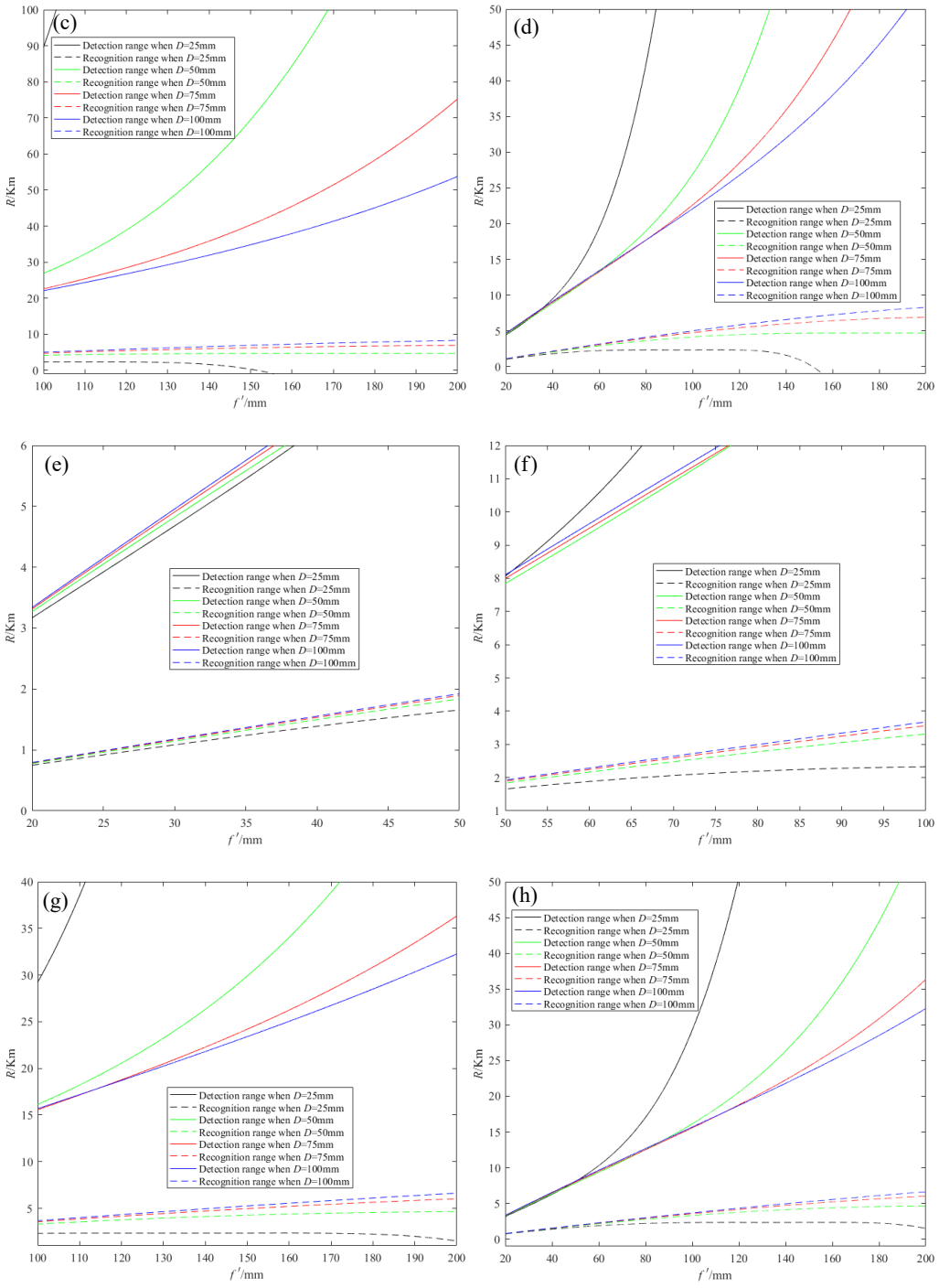

Fig. 5. Continued.

with the increase of focal length and the decrease of detector size. The influence of clear aperture on target acquisition range is more complex. For the detection, when the focal length is small, the smaller is the clear aperture, the smaller is the detection range, as shown in Figs. 5(a) and (e); when the focal length is larger, the smaller is the clear aperture, the greater is the detection range, as shown in Figs. 5(c) and (g). For the recognition, the smaller the clear aperture, the smaller the recognition range. The different trends of detection range and recognition range with the change of clear aperture indicate that the influence of clear aperture on detection and recognition is different.

Figure 6 shows the target acquisition range of the LWIR imaging system under the limitation of F. It is found that the F has a great influence on the target acquisition

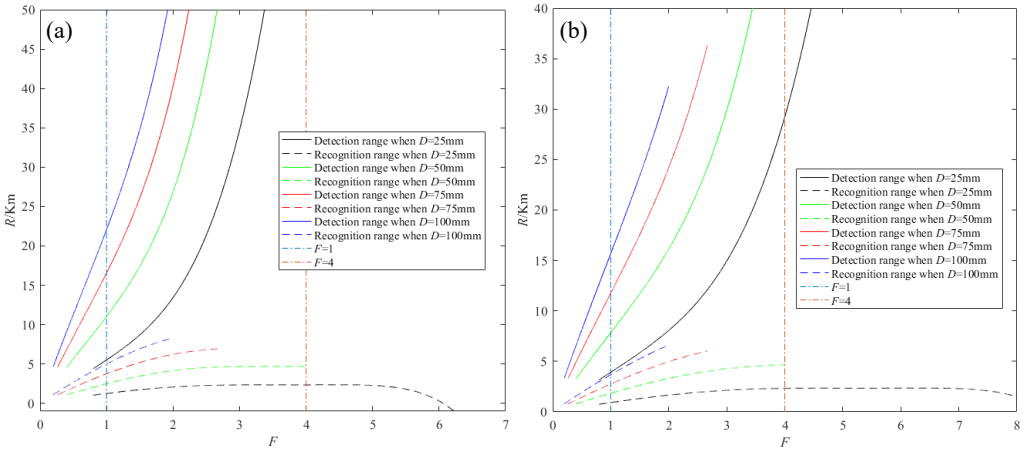

Fig. 6. Relationship between the target acquisition range of the LWIR imaging system and the F number. (a) d_{LWIR} = 12 μm, and (b) d_{LWIR} = 17 μm.

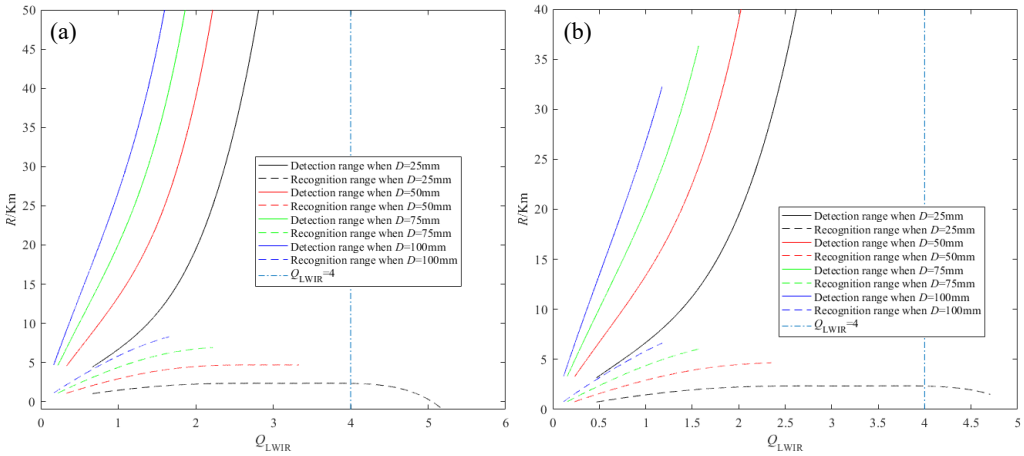

Fig. 7. Relationship between the target acquisition range of the LWIR imaging system and the comprehensive resolution. (a) d_{LWIR} = 12 μm, and (b) d_{LWIR} = 17 μm.

range of the LWIR imaging system with small aperture diameter when compared with Fig. 5.

Figure 7 shows how the target acquisition range changes with the comprehensive resolution Q_{LWIR}. It can be seen from Fig. 7 that with the increase of Q_{LWIR}, the detection and recognition range increases; when $2 < Q_{\mathrm{LWIR}} \leq 4$, the recognition range almost no longer increases, but the detection range still increases. When $Q_{\mathrm{LWIR}} > 4$, the wrong result is obtained because the conditions for applying the model are not met.

The combined effect of F and Q_{LWIR} on the target acquisition range can be illustrated in Fig. 8. In Fig. 8, the Q_{LWIR} is limited to 0.5 to 2, and the corresponding F is about 0.5 to 3.5. Figure 8 shows that with the decrease of the comprehensive resolution, the minimum detection range and the maximum recognition range are getting closer and closer. However, the target acquisition range is decreasing.

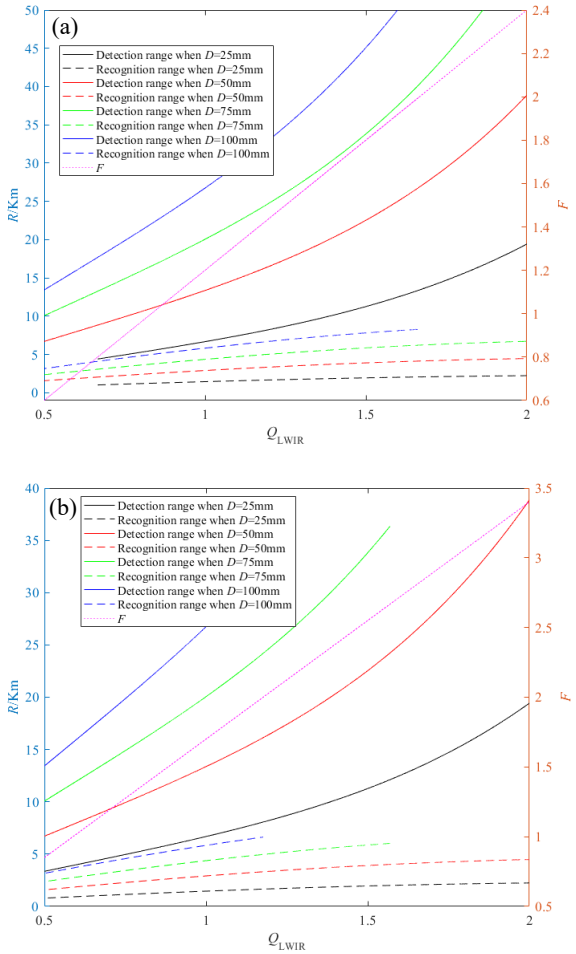

Fig. 8. Target acquisition range of the LWIR imaging system under the limit of Q_{LWIR} and F. (a) d_{LWIR} = 12 μm, and (b) d_{LWIR} = 17 μm.

4.2. Relationship between detection range and recognition range of dual FOV LWIR imaging system

From Eq. (3), the difference between the detection range and the recognition range of the dual FOV LWIR imaging system can be obtained as $\delta_{\mathrm{R\_LWIR}}$

$$\delta_{\mathrm{R\_LWIR}} \approx \frac{W_{\mathrm{T}} K}{\lambda_{\mathrm{LWIR}}} \left(\frac{D_{\mathrm{D}} V_{\mathrm{FOM\_D\_LWIR}}}{N_{\mathrm{D}}} - \frac{D_{\mathrm{R}} V_{\mathrm{FOM\_R\_LWIR}}}{N_{\mathrm{R}}} \right) \tag{13}$$

where $V_{\mathrm{FOM\_D\_LWIR}}$ and $V_{\mathrm{FOM\_R\_LWIR}}$ are the FOMs of detection and recognition of LWIR imaging system, respectively.

Based on the characteristics of the common aperture optical system and the condition that the detection range of the visible imaging system is equal to the recognition range, the Eq. (13) can be written as follows:

$$\delta_{\mathrm{R\_LWIR}} \approx \frac{W_{\mathrm{T}} K}{\lambda_{\mathrm{LWIR}}} \frac{D_{\mathrm{D}}}{N_{\mathrm{D}}} (V_{\mathrm{FOM\_D\_LWIR}} - 1.1\, V_{\mathrm{FOM\_R\_LWIR}}) \tag{14}$$

5. Experiment

5.1. Experimental principle

The experimental principle of performance evaluation of dual FOV common-aperture dual-band imaging system is shown in Fig. 9. The blackbody radiation passing through the LWIR target and the visible source radiation reflected by the visible target enter the off-axis reflective collimator, then pass through the collimator into the common aperture of visible and LWIR optical system and image on the visible and LWIR detector array. After photoelectric conversion, an electronic image is formed and a viewable image is displayed to the observer after computer processing and electro-optic conversion of the display. The contrast of visible target and LWIR target is 0.25 and 3 K, respectively, the size of target is 3.11 mm, and the contrast of target display is 0.2. Based on the previous discussion and the relationship between detection and recogni-

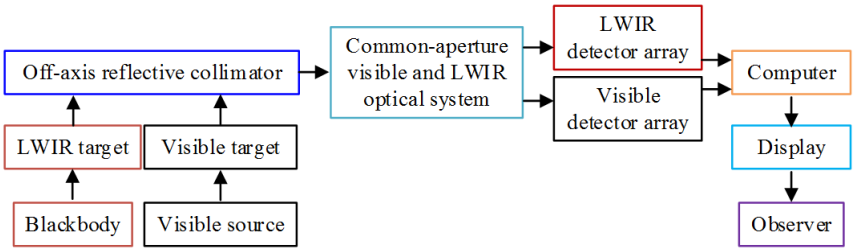

Fig. 9. Experimental principle of performance evaluation of dual FOV common-aperture dual-band imaging system.

T a b l e 2. Optical system parameters.

	First set		Second set	
	Detection	Recognition	Detection	Recognition
f' [mm]	25	105	35	147
D [mm]	25	105	25	105
F	1	1	1.4	1.4

tion in Table 1, the parameters of the optical system used in the experiment are shown in Table 2.

5.2. Theoretical calculation and experimental results

5.2.1. The target acquisition range and the difference between detection range and recognition range of visible imaging system

For the visible imaging system with detector sizes of 3.5 and 5 μm, the two sets of optical system parameters for detection and recognition in Table 2 are selected. The theoretical

T a b l e 3. Comprehensive resolution, target acquisition range and difference between detection range and recognition range of visible imaging system (theoretical/experimental).

	d_V = 3.5 μm		d_V = 5 μm	
	First set	Second set	First set	Second set
Q_V	0.16	0.22	0.11	0.15
R_{D_V} [m]	20.73/19.50	29.02/28.65	14.51/13.84	20.31/19.80
R_{R_V} [m]	20.73/19.45	29.02/28.59	14.51/13.80	20.31/19.75
δ_{R_V} [m]	0/0.05	0/0.06	0/0.04	0/0.05

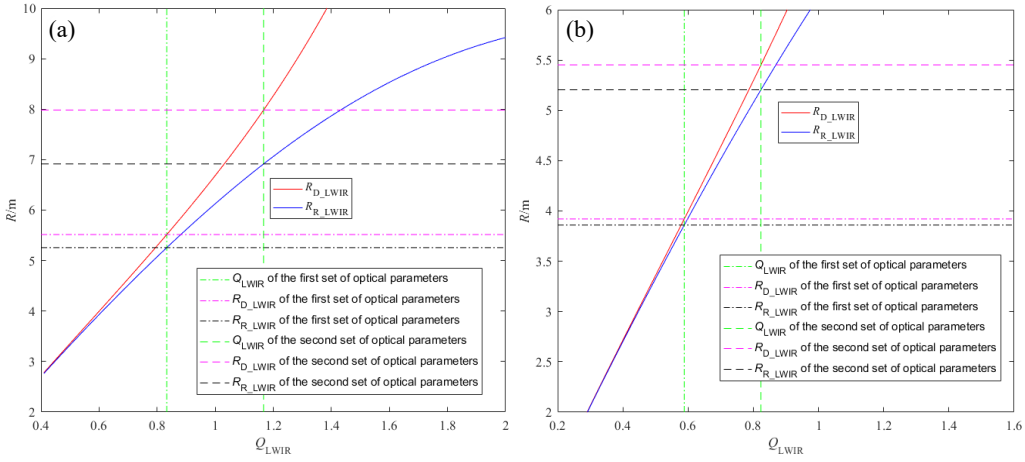

Fig. 10. Relationship of the difference between the detection range and the recognition range and Q_{LWIR}. (a) d_{LWIR} = 12 μm, and (b) d_{LWIR} = 17 μm.

and experimental results are shown in Table 3. In Table 3, R_{D_V}, R_{R_V} and the difference between detection range and recognition range δ_{R_V} have two values, respectively. The values before "/" are the results of theoretical calculation results, and the values after "/" are experimental results. The experimental result is the average of multiple experiments.

5.2.2. The target acquisition range and the difference between detection range and recognition range of LWIR imaging system

The relationship between the target acquisition range and the difference between the detection range and the recognition range and the comprehensive resolution of the LWIR imaging system drawn based on the parameters in Table 2 is shown in Fig. 10.

Table 4 shows the target acquisition range R_{D_LWIR} and R_{R_LWIR} and the difference δ_{R_LWIR} between the detection range and the recognition range corresponding to the two comprehensive resolutions under the two detector sizes.

T a b l e 4. Comprehensive resolution, target acquisition range and difference between detection range and recognition range of LWIR imaging system.

	d_{LWIR} = 12 μm		d_{LWIR} = 17 μm	
	First set	Second set	First set	Second set
Q_{LWIR}	0.83	1.17	0.59	0.82
R_{D_LWIR} [m]	5.51/5.1	7.98/7.51	3.92/3.72	5.45/5.00
R_{R_LWIR} [m]	5.26/4.5	6.92/6.20	3.86/3.62	5.20/4.42
δ_{R_LWIR} [m]	0.25/0.6	1.06/1.31	0.06/0.1	0.25/0.58

5.3. Analysis of results

The theoretical calculation results and experimental results in Table 3 show that the target acquisition range increases with the increase of Q_V; the difference between the detection range and the recognition range also increases. The experimental result of the target acquisition range is smaller than the theoretical result. It is because the experimental results are affected by other factors such as SNR. When the condition that the detection range and the recognition range are equal is met, the detection range and the recognition range are theoretically equal, but the experimental results show that there is a small deviation between the two ranges, which means that the experimental result of the difference between the detection range and the recognition range is larger than the theoretical result. This is because the condition of equality is obtained under the approximate formula of the target acquisition range, which is not exactly the same as the actual situation.

Table 3 and Fig. 10 show that when the optical parameters common to the visible imaging system are used, the comprehensive resolution of detection and recognition of the LWIR imaging system is the same. However, the detection range and recognition range are not equal. Besides, with the increase of the comprehensive resolution, the difference between the two ranges is increasing.

After comparing Table 3 with Table 4, it is found that the target acquisition range of the LWIR imaging system is smaller than that of the visible imaging system, but the difference between the detection range and the recognition range is larger than that of the visible imaging system.

6. Conclusions

When a dual FOV common-aperture dual-band imaging system is modeled and evaluated, it is necessary to consider that the imaging system has a large target acquisition range, and it is necessary to consider the detection range and the recognition range as much as possible. Due to the difference in wavelength, detector size, focal length and the clear aperture, the comprehensive resolution is different, which leads to the difference in the target acquisition range of the visible imaging system and the LWIR imaging system, which further affects the equal interval of detection range and recognition range under the condition of dual FOV. The theoretical and experimental result show that with the increase of comprehensive resolution, the target acquisition range increases, but the difference between detection range and recognition range also increases. Under the condition that the detection range and recognition range of the visible imaging system are equal, and because the comprehensive resolution of the infrared imaging system is much larger than that of the visible imaging system, the difference between the detection range and the recognition range of the infrared imaging system is also larger than that of the visible imaging system.

This study does not consider the effects of atmospheric transmittance and SNR on the target acquisition range and the difference between detection range and recognition range of dual FOV common-aperture dual-band imaging system. This will be the following research subject.

References

[1] Mengshi Li, Yanwei Chen, *Dual-band fire image fusion algorithm based on NSST and feature weighting*, Proc. SPIE 11911, 2nd International Conference on Computer Vision, Image, and Deep Learning, article no. 119111Q (5 October 2021), DOI: 10.1117/12.2604701.

[2] Laborde V., Loicq J., Habraken S., Kershen G., *Making compact and innovative dual-band thermal imagers using hybrid optical elements*, Proc. SPIE 11852, International Conference on Space Optics — ICSO 2020, article no. 118522E (11 June 2021), DOI: 10.1117/12.2599377.

[3] Qing Lin, Weiqi Jin, Hong Guo, Yingzhao Zhang, Maozhong Li, *Confocal-window telescope objective design in visible and long-wave infrared*, Guangxue Xuebao/Acta Optica Sinica **32**(9), 2012, article no. 0922005, DOI: 10.3788/AOS201232.0922005.

[4] Yi-dong Wang, Wen-qiang Li, Qing-bin Meng, *Design of a visible light/LWIR dual-band mutual path optical system*, Electronics Optics & Control **25**(12), 2018, pp. 94–97.

[5] Ting Sun, Haiyan Zhu, Zijian Yang, Xuanzhi Zhang, Huamei Yang, *Design of dual-band common aperture camera optical system*, Journal of Applied Optics **38**(3), 2017, pp. 348–351, DOI: 10.5768/JAO201738.0301002.

[6] Zhanpeng Ma, Yaoke Xue, Yang Shen, Chunhui Zhao, Canglong Zhou, Shangmin Lin, Hu Wang, *Design and realization of visible/LWIR dual-color common aperture optical system*, Guangzi Xuebao/Acta Photonica Sinica **50**(5), 2021, article no. 0511002, DOI: 10.3788/gzxb20215005.0511002.

[7] HAIBIN ZHU, YU SHAO, YUANJIAN ZHANG, LIANG ZHOU, ZHIGANG XU, DALUE ZHU, JUNJING SHAN, *Optical system design of visible/infrared and double-FOV panoramic aerial camera*, Journal of Applied Optics **38**(1), 2017, pp. 7–11, DOI: 10.5768/JAO201738.0101002.

[8] VOLLMERHAUSEN R.H., JACOBS E.L., DRIGGERS R.G., *New metric for predicting target acquisition performance*, Optical Engineering **43**(11), 2004, pp. 2806–2813, DOI: 10.1117/1.1799111.

[9] SHORT R., DRIGGERS R., LITTLEJOHN D., SCHOLTEN M., *Performance benefits of small-pitch, high-dynamic-range, digitally restored infrared imaging systems using triangle orientation discrimination and NVIPM*, Applied Optics **58**(23), 2019, pp. 6315–6320, DOI: 10.1364/AO.58.006315.

[10] HIXSON J.G., TEANEY B.P., GRAYBEAL J.J., NEHMETALLAH G., *Analysis and modeling of observer performance while using an infrared imaging system*, Optical Engineering **59**(3), 2020, article no. 033106, DOI: 10.1117/1.OE.59.3.033106.

[11] FIETE R.D., *Modeling the Imaging Chain of Digital Cameras*, SPIE Press, 2010, DOI: 10.1117/3.868276.

[12] FIETE R.D., *Image quality and λFN/p for remote sensing systems*, Optical Engineering **38**(7), 1999, pp. 1229–1240, DOI: 10.1117/1.602169.

[13] HOLST G., *Imaging system performance based upon Fλ/d*, Optical Engineering **46**, 2007, article no. 103204, DOI: 10.1117/1.2790066.

[14] DRIGGERS R., GORANSON G., BUTRIMAS S., HOLST G., FURXHI O., *Simple target acquisition model based on Fλ/d*, Optical Engineering **60**(2), 2021, article no. 023104, DOI: 10.1117/1.OE.60.2.023104.

Received November 17, 2021
in revised form February 21, 2022